Prevention of acute graft-versus-host disease by blocking T-cell entry to secondary lymphoid organs

Andreas Beilhack,[1,2] Stephan Schulz,[1,3] Jeanette Baker,[1] Georg F. Beilhack,[4] Ryosei Nishimura,[1] Enosh M. Baker,[1] Gilad Landan,[1] Edward I. Herman,[1] Eugene C. Butcher,[5] Christopher H. Contag,[6] and Robert S. Negrin[1]

[1]Department of Medicine, Stanford University, Stanford, CA; [2]Department of Medicine II, Würzburg University, Würzburg, Germany; [3]Department of Pathology, Technical University München, München, Germany; [4]Department of Medicine I, Ulm University, Ulm, Germany; and Departments of [5]Pathology and [6]Pediatrics, Stanford University, Stanford, CA

In acute graft-versus-host disease (aGVHD), donor T cells attack the recipient's gastrointestinal tract, liver, and skin. We hypothesized that blocking access to distinct lymphoid priming sites may alter the specific organ tropism and prevent aGVHD development. In support of this initial hypothesis, we found that different secondary lymphoid organs (SLOs) imprint distinct homing receptor phenotypes on evolving alloreactive effector T cells in vivo. Yet preventing T-cell entry to specific SLOs through blocking monoclonal antibodies, or SLO ablation, did not alter aGVHD pathophysiology. Moreover, transfer of alloreactive effector T cells into conditioned secondary recipients targeted the intestines and liver, irrespective of their initial priming site. Thus, we demonstrate redundancy of SLOs at different anatomical sites in aGVHD initiation. Only prevention of T-cell entry to all SLOs could completely abrogate the onset of aGVHD. (Blood. 2008;111:2919-2928)

Introduction

Allogeneic hematopoietic cell transplantation (aHCT) is a successful therapy for malignant and nonmalignant diseases. The major limitations of this treatment modality are opportunistic infections and aGVHD, an immune syndrome caused by donor T cells that recognize recipient tissues as foreign. A hallmark of aGVHD is the specific organ injury affecting primarily the gastrointestinal tract (GIT), liver, and skin.[1,2] Recently, we and others have demonstrated in murine models across major histocompatibility barriers that, similar to other adaptive immune responses,[3-5] aGVHD is initiated exclusively in the T-cell areas of secondary lymphoid organs (SLOs) during the first 3 days after aHCT.[2,6] SLOs, including the spleen, lymph nodes (LN), Peyer's patches (PPs), and other mucosa-associated lymphatic tissues, enable interactions between antigen presenting cells (APCs) and T lymphocytes through tightly regulated compartmentalization.[3-5] Antigen-specific T cells encountering activated APCs proliferate and differentiate into effector T cells. One possible explanation for the specific organ manifestation in aGVHD is that alloreactive effector T cells are instructed in lymphoid organs to migrate to corresponding target tissues. Several findings support this concept, suggesting that homing properties of T cells are imprinted during the initiation of an immune response.[7-13] For example, T cells having encountered cognate antigen in gut-associated lymphatic tissues (GALT) would be instructed to migrate to the intestinal tract where the likelihood of encountering the antigen is the highest.[8,11,12] Similarly, T cells encountering antigen in a skin draining LN would favorably migrate to the skin.[8,14] Host type APCs are pivotal in aGVHD induction,[15] and in other murine models it was demonstrated that dendritic cells (DCs), as potent APCs, can mediate the selective generation of intestinal effector T cells in GALT and skin-homing effector T cells in skin draining LNs, respectively.[9-12,16,17] Furthermore, retinoic acid, abundant in the intestinal tract but virtually absent in the skin, promotes intestinal trafficking of T cells via their retinoic acid receptors.[18] Others reported that PP-deficient mice did not develop lethal aGVHD in contrast to wild-type (WT) animals.[19] Accordingly, when access of alloreactive donor cells to PPs was prevented with MAdCAM-1 blocking antibodies or by using $CCR5^{-/-}$-deficient donor animals, recipients were protected from aGVHD. Taken together, these data suggested that distinct priming sites may be responsible for the specific target organ manifestation in aGVHD. However, it remained to be tested whether certain aGVHD initiation sites instruct alloreactive T-cell trafficking or whether aGVHD target tissues selectively attract alloreactive T cells.[20]

Therefore we tested in various in vivo scenarios whether the lack of potential instructive priming sites would reduce or delay infiltration of aGVHD target tissues after aHCT. Blocking entry to selected SLOs by monoclonal antibodies (MAbs) or by lymphoid ablation did not alter the aGVHD manifestation. Furthermore, alloreactive effector cells isolated from anatomically distinct

Submitted September 25, 2007; accepted October 23, 2007. Prepublished online as *Blood* First Edition paper, November 7, 2007; DOI 10.1182/blood-2007-09-112789.

A.B. and S.S. contributed equally to this study.

An Inside *Blood* analysis of this article appears at the front of this issue.

The online version of this article contains a data supplement.

The publication costs of this article were defrayed in part by page charge payment. Therefore, and solely to indicate this fact, this article is hereby marked "advertisement" in accordance with 18 USC section 1734.

aGVHD initiation sites migrated efficiently to the intestinal tract and liver, irrespective of their original priming site. Thus, we demonstrate that SLOs as priming sites are redundant in aGVHD initiation. Ultimately, blocking T-cell entry to all SLOs was required to prevent aGVHD.

Methods

Mice

FVB/N (H-2^q, Thy1.1), Balb/c (H-2^d, Thy1.2), C57Bl/6 (H-2^b, Thy1.2), and C57Bl/6-Lymphotoxin-α-receptor-deficient (B6-LTα$^{-/-}$) mice[21] were purchased from Jackson Laboratories (Bar Harbor, ME). Peyer's patch–deficient Balb/c (PP^{KO}) mice were generated by the timed intravenous injection of pregnant mice with 100 μg lymphotoxin-β-receptor IgG fusion protein (LTβR-IgG, a kind gift from Dr J. L. Browning, Biogen, Cambridge, MA) on gestational day E17.5 and subsequently of the newborns intraperitoneally within 12 hours postpartum.[22,23] Depletion of PPs was confirmed macroscopically and by histology in littermates and for each mouse at termination of the experiment. The luciferase expressing (*luc*$^+$) transgenic FVB/N line was generated as previously described.[2,24,25] Either female heterozygous or homozygous *luc*$^+$ offspring of the transgenic founder line FVB-L2G85 were used for transplantation experiments. All animal studies were performed under institutional approval according to specific animal use protocols.

Flow cytometric cell purification and analysis

Unless otherwise indicated, the following antibodies were purchased from eBiosciences (San Diego, CA) and BD Pharmingen (San Diego, CA) for FACS analysis on an LSR flow cytometer (Becton Dickinson, Mountain View, CA): CD3ϵ (145-2c11), CD4 (RM4-5), CD8α (53-6.7), CD11b/Mac-1 (M1/70), CD25 (PC61), CD44 (IM7), CD45R/B220 (RA3-6B2), CD62L (MEL14), CD69 (H1.2F3), CD103/αEβ7, CCR5 (C34-3448), CCR9 (242503, R&D Systems, Minneapolis, MN), CXCR3 (220803, R&D Systems), Gr-1 (RB6-8C5), H-2Kq (KH114), H-2Dq (KH117), H-2Dd (34-2–12), LPAM-1/α4β7 (DATK32), NK1.1 (PK136), P-selectin ligand-IgG fusion protein, E-selectin-ligand-IgG fusion protein, anti–human-IgGκ-PE (Jackson ImmunoResearch Laboratories (West Grove, PA), Thy1.1 (H1S51), Thy1.2 (53-2.1). Dead cells were excluded by propidium iodide staining shortly before FACS.

For transplantation of T-cell subsets, splenic single cell suspensions from *luc*$^+$ FVB-L2G85 mice were enriched with CD4- and CD8-conjugated magnetic beads using the AutoMACS system (Miltenyi Biotech, Auburn, CA). Cell purity was confirmed by postenrichment fluorescence-assisted cell sorting (FACS) analysis ($>85\%$). FACS analyses were performed on single cell suspensions from cervical LNs (cLNs), inguinal LNs (iLNs), mesenteric LNs (mLNs), PP, and spleen at indicated time points after aHCT. For cell-proliferation analysis, splenocytes (10^7/mL) were resuspended in PBS and Vybrant CFDA SE Tracer reagent (Invitrogen, Carlsbad, CA) at a final concentration of 5 μM for exactly 6 minutes at 37°C. Immediately after staining, cells were washed in 5 volumes of ice-cold RPMI plus 10% fetal bovine serum (FCS; Invitrogen) twice, resuspended in PBS and counted before intravenous injection. Flow cytometric data were analyzed with FlowJo Software (TreeStar, Ashland, OR).

Allogeneic HCT

To condition mice for aHCT, a Phillips Unit Irradiator (250 kv, 15 milliamperes) was used to deliver lethal radiation on day 0 relative to transplantation. Female 8- to 12-week-old HCT recipient mice received split doses of either 400 Gy (allogeneic Balb/c recipients, 2×400 rad) or 4.5 Gy (allogeneic C57Bl/6, B6-LTα$^{-/-}$ recipients, 2×400 rad) 3 to 4 hours apart. For hematopoietic reconstitution, animals were injected with 5×10^6 FVB/N wild-type BM cells intravenously within 3 hours after the second dose of radiation. To induce aGVHD, wild type mice were coinjected intravenously with FVB/N-L2G85 4×10^6 *luc*$^+$ splenocytes.

In vivo bioluminescence imaging and ex vivo imaging analysis

In vivo bioluminescence imaging (BLI) was performed as previously described, using an IVIS100 CCD-imaging system (Xenogen, Alameda, CA).[2,24] After in vivo BLI, mice were injected intraperitoneally with an additional dose of luciferin (150 μg/g bodyweight). Five minutes later animals were killed. Selected tissues were prepared and imaged for 5 minutes. Tissue processing was timed to stay within a period of 3 minutes. Ex vivo imaging resulted in high-resolution images displaying signal foci within organs of interest and directed the embedding of tissues for histology as well as cell extraction for FACS analysis. Imaging data were analyzed and quantified with Living Image Software (Xenogen) and Igor (WaveMetrics, Lake Oswego, OR).

In vivo antibody administration and splenectomies

Recipient Balb/c or B6-LTα$^{-/-}$ mice were splenectomized and controls sham operated 2 weeks before aHCT, according to standard protocols. In initial experiments mice received a single dose of either 150 μg purified anti-MAdCAM-1 (αMAdCAM-1, MECA-367) or isotype control MAbs intravenously. In subsequent experiments aHCT recipients received either αMAdCAM-1 (MECA-367) or anti-L-selectin (αCD62L, Mel-14) MAbs alone or in combination, or rat IgG2a isotype control MAbs intravenously as follows: day 0 immediately before cell injection, 150 μg; day 1 to 4, 100 μg; day 5, 50 μg. Antibodies were either purified from hybridomas at Stanford University or purchased from eBioscience.

Transfer experiments into secondary aHCT recipients

Primary aHCT Balb/c recipients were conditioned with 2 split doses of 4 Gy (2×400 rad) and transplanted with magnetic-assisted cell sorting (MACS)–purfied *luc*$^+$ FVB-L2G85 splenocytes as described in "Allogeneic HCT." On day 3 after aHCT, cells were isolated from mLN or peripheral LNs (pLNs) (cLN and iLN) and 10^7 *luc*$^+$ Thy1.1$^+$ T cells were injected intravenously into secondary Balb/c recipients that were conditioned (2×4 Gy) and transplanted with WT FVB/N cells at the same time as the primary recipients (day 0). To study the short term homing of alloreactive T cells without biasing secondary migration effects, secondary recipients were imaged within 18 hours after secondary transfer.

Histology

Tissues were sampled over the time course of 6 days and cryopreserved at −80°C. Fresh frozen 5-μm-thick sections were mounted on positively charged precleaned microscope slides (Superfrost/Plus; Fisher Scientific, Pittsburgh, PA) and stored at −80°C. The sections were initially thawed for 20 minutes at room temperature (RT). After acetone fixation (7 minutes at RT) and air drying (3 minutes), sections were incubated with blocking solution (PBS + 2% FCS) for 15 minutes. Incubations with primary antibodies were performed for 1 hour at RT. Directly conjugated antibodies were used for lineage determination of T lymphocytes (CD8-FITC and CD4-PE; BD Pharmingen) and diluted 1:200 in 1× PBS. The donor T-cell marker Thy1.1-APC (BD Pharmingen) was used at a dilution of 1:100 in PBS. Nuclei were stained with DAPI. Washing steps after antibody incubation and 4,6-diamidino-2-phenylindole (DAPI) staining were performed in 1× PBS (3 times, 3 minutes each). Fluorescence microscopic evaluation was performed on a Nikon microscope (Eclipse, TE 300). Microscopic photos were obtained using a digital camera (Spot; Diagnostic Instruments, Sterling Heights, MI). Digital images were saved in TIFF and inserted and processed in PowerPoint (Microsoft, Redmond, WA). Standard magnifications were 200×/0.45 NA and 400×/0.60 NA.

Statistical analyses

Data were compared using GraphPad Prism 4.0c (GraphPad Software, San Diego, CA) by log rank test, Student *t* test, Kruskal-Wallis test, or 2-way ANOVA with Bonferroni correction, as appropriate. Data represent mean values, error bars indicate 1 SD, and *P* values less than .05 were deemed statistically significantly different.

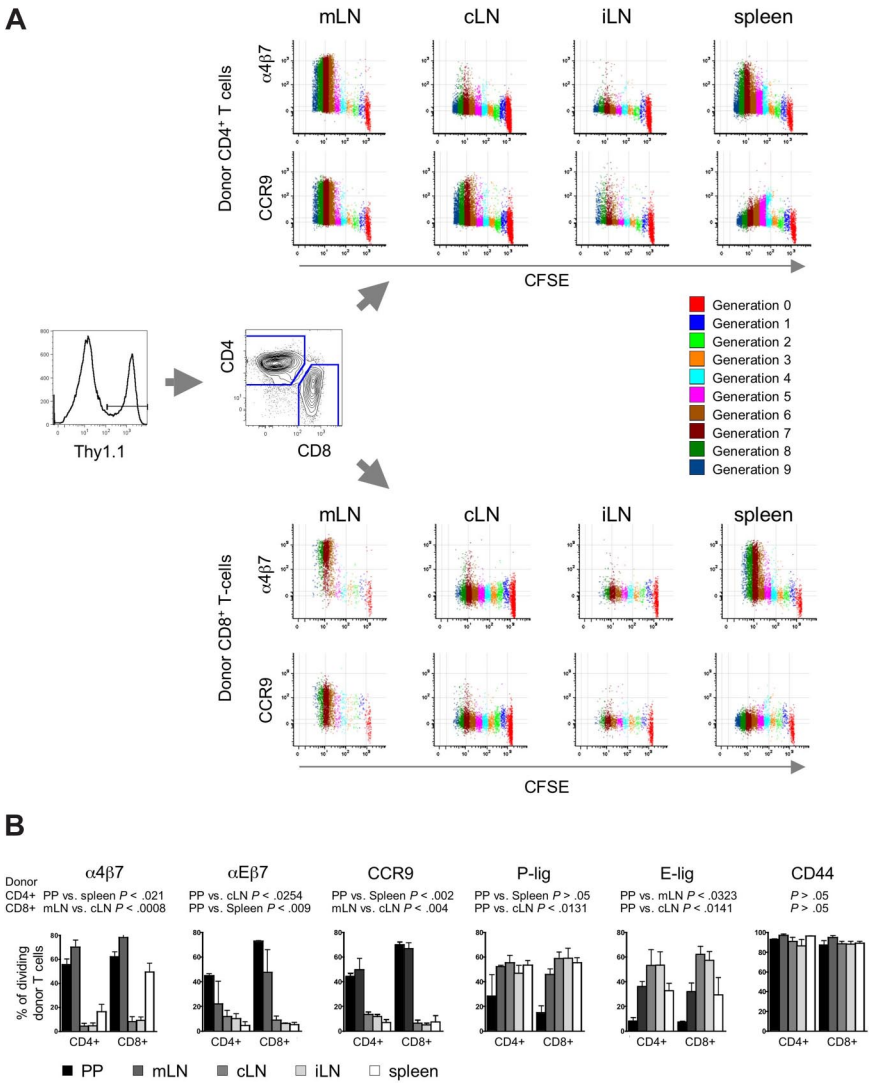

Figure 1. Differential homing receptor expression by alloreactive T cells in anatomic distinct priming sites. CFSE-labeled allogeneic FVB/N-L2G85 (H-2^q, Thy1.1) splenocytes were transplanted into myeloablative conditioned Balb/c recipients (H-2^d, Thy1.2). On day 3 after aHCT, immediately before alloreactive T cells enter aGVHD target organs, cells were isolated from different SLOs for phenotypic comparison by flow cytometry. (A) Representative staining of α4β7 integrin and CCR9 on in vivo primed Thy1.1$^+$ donor CD4$^+$ T cells (top) and CD8$^+$ T cells (bottom). Alloreactive T cells had undergone several cell divisions (color encoded) and markedly up-regulated α4β7 integrin and CCR9 after 5 cell divisions predominantly in mLN and spleen (1 of 4 representative experiments is shown). (B) Bar graphs depict percentage of dividing donor T cells expressing peripheral homing receptors. Of note, intestinal-associated lymphoid organs (PP, mLN) up-regulated mucosal-associated homing receptors, whereas pLNs (cLN and iLN) displayed more pronounced skin homing receptor expression (E-lig, P-lig). Most of the dividing cells in all SLO are CD44$^+$. Cells were pooled from 5 mice, 3 independent experiments were performed. Bars depict means plus or minus SD.

Results

Differential expression of homing receptors in secondary lymphoid organs during aGVHD initiation

To explore the role of different SLOs in the aGVHD organ manifestation, we analyzed the acquisition of homing receptors on alloreactive T cells. Therefore, myeloablatively conditioned Balb/c recipients (H-2^d, Thy1.2$^+$) received transplants of FVB/N bone marrow (BM) cells plus CFSE-labeled luciferase transgenic (*luc*$^+$) FVB/N-L2G85 splenocytes as a source of alloreactive T cells (H-2^q, Thy1.1$^+$). On day 3 after transplantation, the last time point before alloreactive T cells exit SLOs, bioluminescence imaging guided the extraction of *luc*$^+$ donor cells from different SLOs, namely Peyer's patches (PP), mesenteric LN (mLN), spleen, cervical LN (cLN), and inguinal LN (iLN) as peripheral LN (pLNs) to characterize donor-derived T-cell populations. Thy1.1$^+$ donor T cells were found to have undergone multiple divisions in SLOs as indicated by the dilution of CFSE (Figure 1A).

Next we analyzed expression of homing receptors that have been implicated in organ-specific effector cell trafficking.[13] Dividing CD4$^+$ and CD8$^+$ donor T cells of PP and mLN (but not the pLNs) up-regulated the gut homing receptors α4β7-integrin,[8] αEβ7 (CD103),[26] and CCR9[27,28] (Figure 1A,B). α4β7^{hi} donor CD8$^+$ T cells were also found in the spleen. Donor T cells in pLNs up-regulated more E-selectin ligand (E-lig), associated with skin homing, than did T cells of PP, mLN, and spleen. Similarly P-selectin ligand (P-lig) was more pronounced in pLNs than in PP. However, more than 90% of dividing donor T cells expressed the activation marker CD44 in all aGVHD initiation sites (Figure 1B), thus T-cell proliferation and activation per se were comparable in all SLOs analyzed. These results were consistent with previous in vitro and in vivo observations of several independent investigators in different models of other adaptive immune responses[7-11,17] supporting the concept of existing instructive sites in aGVHD initiation.

Peyer's patches are important but not essential sites in aGVHD induction

Bioluminescent signals from excised tissues revealed involvement of PP during the initiation phase of aGVHD.[2] These observations and a previous report[19] suggested that gut alloreactive T cells might be specifically instructed in the PP, and depletion of PP may

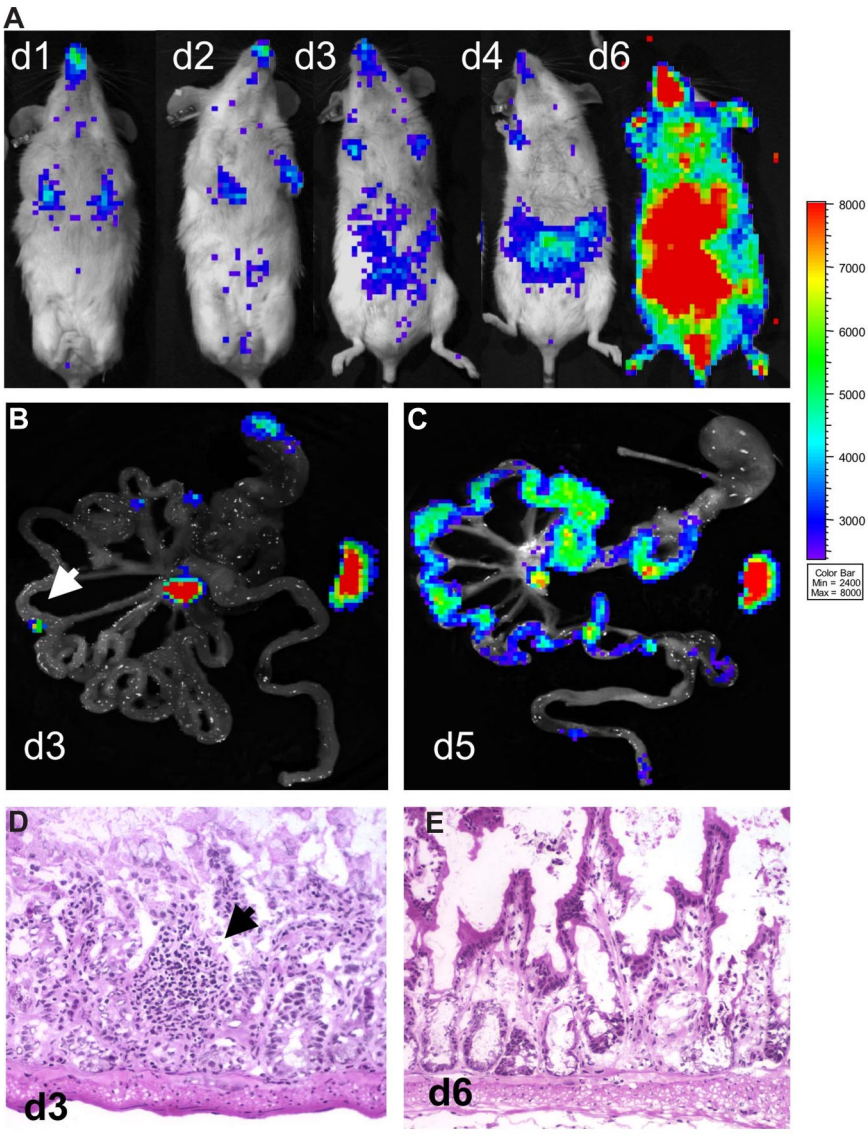

Figure 2. Onset of intestinal aGVHD is not delayed in Peyer's patch (PP^{KO})–deficient mice. Myeloablatively conditioned PP^{KO} Balb/c mice received transplants of *luc*$^+$ FVB/N-L2G85 splenocytes plus FVB/N wild type bone marrow cells. (A) In vivo BLI of transplanted mice showed expansion of alloreactive T cells over lymphatic and intestinal sites by day 4, intestinal, liver, and skin infiltration by day 6 after aHCT. (B) Ex vivo images of the intestinal tract on day 3 displayed BLI signals from the mLN and the spleen. In some animals small light-emitting foci (arrow) were observed, which were sampled and analyzed (see below). (C) Ex vivo imaging of the gastrointestinal tract confirmed diffuse intestinal infiltration by *luc*$^+$ donor cells on day 5. (D) Histologically, above described foci (arrow) were identified as ill-defined small lymphocytic aggregates. All of the analyzed mice were deficient for PP. (E) hematoxylin and eosin (H&E) analysis on day 6 after aHCT revealed a grade 2 GVHD on intestinal samples, showing apoptotic bodies and extensive crypt destructions in PP^{KO} recipients.

ameliorate intestinal aGVHD. Therefore, we generated mice devoid of PP (PP^{KO} mice) by injecting a lymphotoxin-β-receptor IgG fusion protein during embryonic development.[22,23] Analysis of representative mice from each litter confirmed the lack of PP on macroscopic and histologic levels. Surprisingly, aHCT of these myeloablative conditioned Balb/c PP^{KO} recipients with allogeneic *luc*$^+$ splenocytes and WT BM cells resulted in severe and lethal aGVHD with a time course indistinguishable from WT animals. In one representative experiment (of 2), 4 of 11 PP^{KO} aHCT recipients were killed early in the disease course (day 6) for histologic evaluation. The in vivo BLI signals were distributed and increased similarly as in WT Balb/c controls after aHCT (Figure 2A). On day 3 after aHCT, bioluminescent signals from GIT samples of PP^{KO} mice revealed only a few discrete light-emitting foci in the small intestines (Figure 2B). Histologic evaluation of serial sections from these positive foci revealed diffuse and unorganized lymphoid aggregates, and no PP (Figure 2D). Immunofluorescent staining showed that Thy1.1$^+$ donor T-lymphocytes dominated these aggregates (data not shown). Importantly, the strongest BLI signals were detectable in mLN and spleen, indicating predominant alloreactive T-cell expansion at these sites (Figure 2B) in PP^{KO} recipients. PP^{KO} mice and WT mice simultaneously developed intestinal and later skin aGVHD. Strong lymphocytic infiltrates became evident by day 5 after aHCT (Figure 2C) paralleled by tissue injury typical of aGVHD (Figure 2E). FACS analysis demonstrated donor T cells expressing high levels of $\alpha4\beta7^+$ in mLN and spleen of these PP^{KO} mice on day 3 (data not shown). A recent report using a different aHCT model of myeloablatively conditioned PP^{KO} recipients supports our data, again demonstrating that these animals develop aGVHD with a similar time course and severity to WT recipients.[29] Together these results suggest that lymphoid organs other than PP, in particular mLN and spleen, can functionally compensate for the lack of PP by activating alloreactive T cells capable of intestinal aGVHD induction (Table 1).

Mice lacking Peyer's patches and lymph nodes develop aGVHD

Because PP appeared not as the only sites to give rise to gut-tropic alloreactive T cells, we asked whether mice deficient in LNs and PPs would develop aGVHD. Mice deficient in the lymphotoxin-alpha chain (B6-LT$\alpha^{-/-}$) do not develop SLOs, with the exception of a morphologically altered spleen.[21] Either C57Bl/6 wild-type (B6.WT, H-2^b) or B6-LT$\alpha^{-/-}$ (H-2^b) mice received transplants of FVB/N WT BM cells plus *luc*$^+$ splenocytes. The recipients were

Table 1. Redundancy of secondary lymphoid organs in the generation of aGVHD target tissue–specific alloreactive effector T cells

No access to these aGVHD initiaton site(s)	Strategy	aGVHD initiation sites:	aGVHD target manifestation: (+ GIT, + liver, + skin)
PP	Embryonic PP ablation, (LTβ-IgG-fusion protein)	mLN, pLN, spleen*	+++
PP plus mLN plus pLN	Genetic deficiency (LTα-/- mutation)	spleen	+++
PP plus mLN	Anti-MAdCAM-1 blocking antibodies	pLN, spleen	+++
pLN	Anti-CD62L blocking antibodies	mLN, spleen	+++
PP plus mLN plus pLN	Anti-CD62L blocking antibodies + anti-MAdCAM-1 blocking antibodies	spleen	+++
Spleen	splenectomy	PP, mLN, spleen	+++
PP plus mLN plus spleen	Anti-MAdCAM-1 blocking antibodies + splenectomy	pLN	+++
pLN plus spleen	Anti-CD62L blocking antibodies + splenectomy	mLN	+++
PP plus mLN plus pLN plus spleen	*Genetic deficiency (LTα-/- mutation) + splenectomy or anti-CD62L blocking antibodies + anti-MAdCAM-1 blocking antibodies + splenectomy	None§ None	None None
None	Isotype control antibody	PP, mLN, pLN, spleen	+++

MAdCAM-1 indicates mucosal vascular addressin cellular adhesion molecule (MECA-367); CD62L, L-selectin (MEL-14).
*Ectopic ill-defined lymphoid aggregates in intestinal mucosa observed.
§Potential discrete ectopic lymphoid aggregates in intestinal mucosa.
+++ aGVHD manifestation in the gastrointestinal tract (GIT), liver, and skin.

not optimally suited for in vivo imaging due to their light-absorbing skin and coat pigmentation. However, ex vivo imaging of these recipient animals revealed proliferation of *luc*$^+$ alloreactive T cells in SLOs of B6.WT recipients (Figure 3A), similar to the FVB/N into Balb/c aHCT model.[2] In contrast, in B6-LTα$^{-/-}$ mice, *luc*$^+$ donor T cells projected a signal only on the spleen at day 3 (Figure 3B). However, by day 6 both B6.WT and B6-LTα$^{-/-}$ mice developed intestinal aGVHD as shown by the infiltration of *luc*$^+$ donor cells (Figure 3D,E; histology Figure 3G,H). Donor T-cell proliferation in the spleen of B6-LTα$^{-/-}$ mice showed that this organ was sufficient to compensate for the lack of other SLOs. Therefore, we splenectomized B6-LTα$^{-/-}$ mice (B6-LTα$^{-/-}{}_{\text{SplEx}}$) 2 weeks before aHCT, eliminating all SLOs. After myeloablative conditioning, these B6-LTα$^{-/-}{}_{\text{SplEx}}$ mice together with control B6-LTα$^{-/-}$ and B6.WT mice received allogeneic FVB/N *luc*$^+$ splenocytes and WT BM cells. In 3 independent experiments we found that B6-LTα$^{-/-}{}_{\text{SplEx}}$ mice did not develop intestinal aGVHD by day 6 (Figure 3C,F,I) in contrast to B6.WT mice with intact SLOs (Figure 3A,D,G) or B6-LTα$^{-/-}$ mice lacking PPs and LNs (Figure 3B,E,H). Histologic evaluation of skin and liver of B6-LTα$^{-/-}{}_{\text{SplEx}}$ mice did not show alloreactive T-cell infiltration of these sites in contrast to B6-LTα$^{-/-}$ and B6-WT recipients (Figure

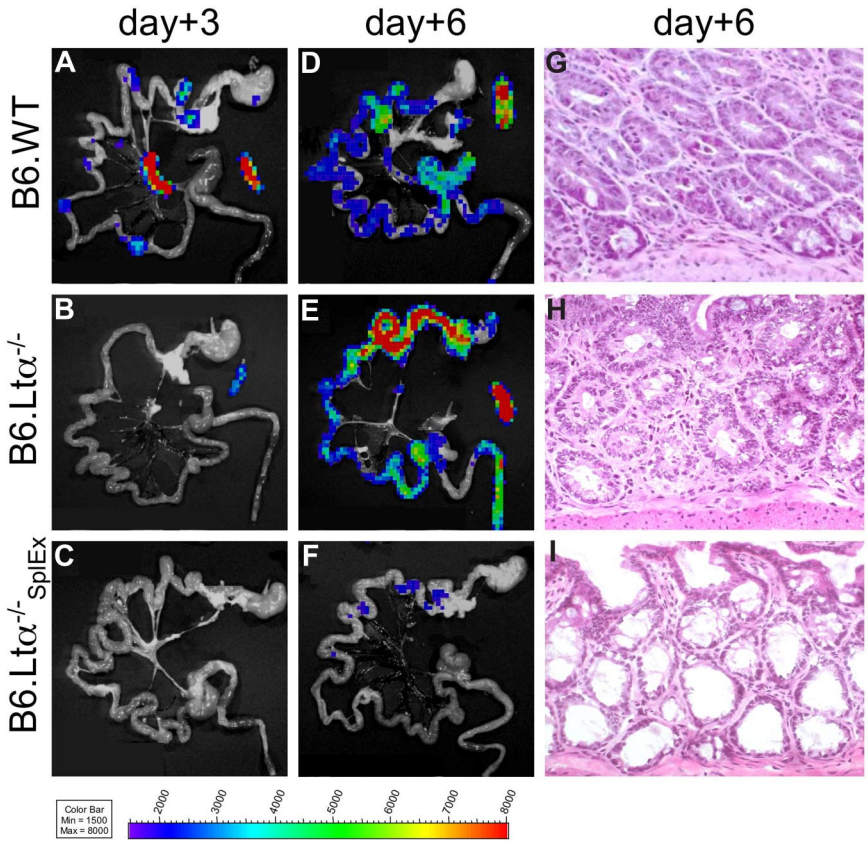

Figure 3. Lymph node– and Peyer's patch–deficient LTα$^{-/-}$ mice develop intestinal aGVHD, while splenectomized LTα$^{-/-}$ mice are protected. Myeloablatively conditioned C57Bl/6 wild-type recipients (B6.WT) were compared with C57Bl/6-Lymphtoxin alpha$^{-/-}$ mice (B6.LTα$^{-/-}$, deficient for PP and LNs) and splenectomized B6.LTα$^{-/-}$ recipients (B6.LTα$^{-/-}{}_{\text{SplEx}}$) after transplantation with allogeneic *luc*$^+$ FVB/N T cells plus WT BM cells. (A) Ex vivo BLI signals projected to the spleen, mLN, and PP in B6.WT mice, solely to the spleen in B6.LTα$^{-/-}$ (B), but were not apparent in B6.LTα$^{-/-}{}_{\text{SplEx}}$ recipients (C) on day 3 after aHCT. (D,E) On day 6 ex vivo BLI signals increased over the intestines in B6.WT and B6.LTα$^{-/-}$ recipients in similar strength, in stark contrast to B6.LTα$^{-/-}{}_{\text{SplEx}}$ recipients (F) Ex vivo imaging correlated well with H&E histopathology on day 6, by showing widespread signs of aGVHD (grade 2) in the small and large bowel of B6.WT (G) and B6.LTα$^{-/-}$ recipients (H). In contrast, the intestinal mucosa of B6.LTα$^{-/-}{}_{\text{SplEx}}$ recipients hardly showed any lymphocytes and no aGVHD (I).

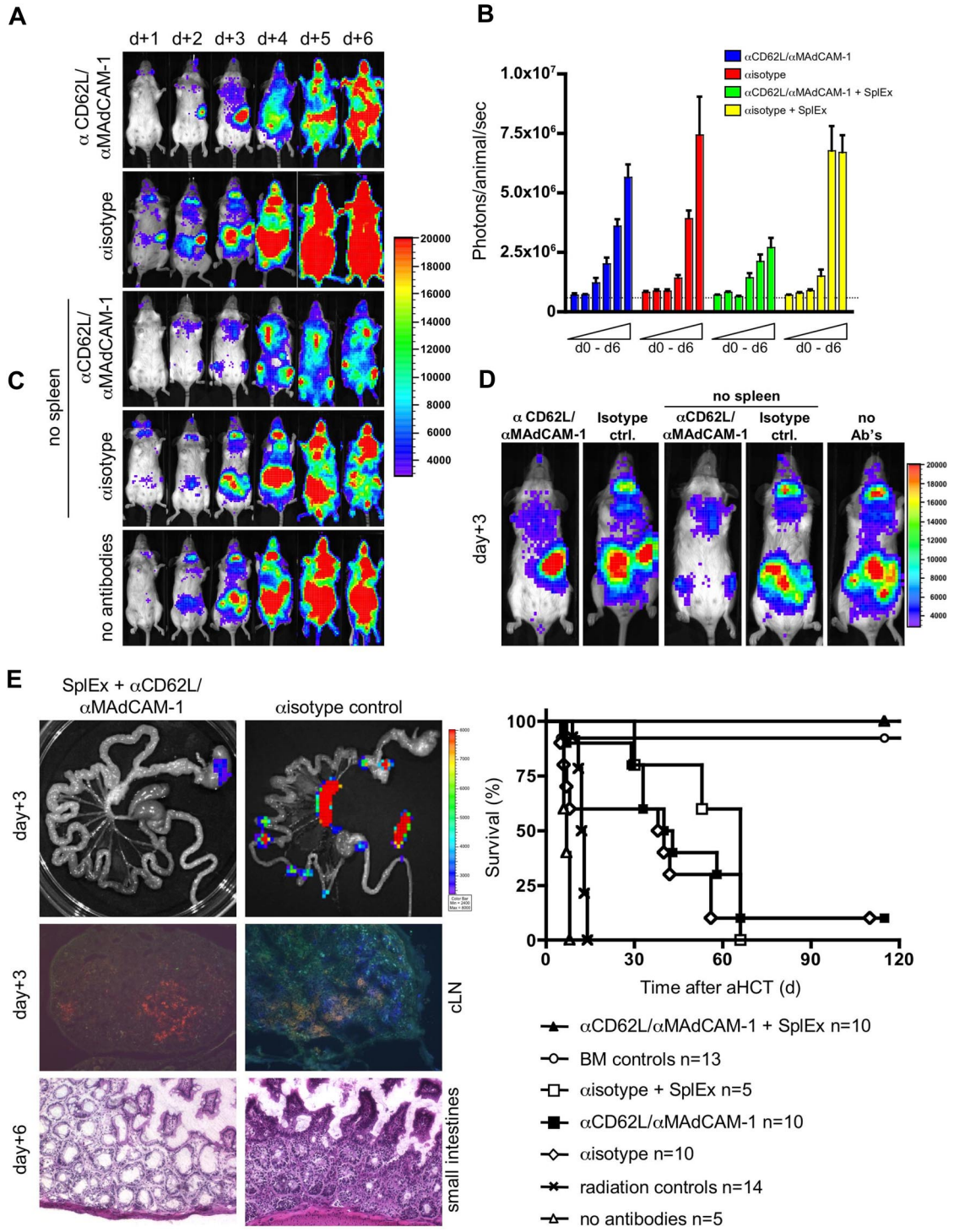

Figure 4. Blocking the access to all SLOs prevents aGHVD. Conditioned Balb/c recipients (H-2^d) received transplants of allogeneic *luc*$^+$ T cells and wild type FVB/N (H-2^q) bone marrow cells. To prevent donor T-cell entry to SLOs either Balb/c or splenectomized Balb/c (no spleen, SplEx) aHCT recipients were intravenously injected daily with αCD62L αMAdCAM-1 or isotype control antibodies. (A) In vivo BLI for the first 6 days after aHCT demonstrated effective blocking of nodal sites by combined αCD62L/αMAdCAM-1 treatment. However, alloreactive cells proliferated in the spleen before aGVHD target infiltration (top panel). Splenectomy plus isotype control antibody treatment lead to compensatory alloreactive cell expansion in remaining accessible sites (second from bottom). However, combined αCD62L/αMAdCAM-1$_{SplEx}$ treatment resulted in less intense BLI signals (middle), that projected predominantly to the bone marrow compartments (sternum, femura and pelvis). By day 4 abdominal sites were targeted in all groups except for the αCD62L/αMAdCAM-1$_{SplEx}$ group. Shown is one representative animal (of 5) from each group (reproduced in 3 independent experiments). (B) The total body photon emission of αCD62L/αMAdCAM-1$_{SplEx}$ recipients is reduced in contrast to all other groups ($P < .015$). This indicates compensatory proliferation in recipients with partially blocked SLO T-cell entry. Means plus or minus SD are shown in the bar graphs. (C) In higher magnification (day 3), BLI reveals the compensatory sites of alloreactive proliferation. The spleen region was positive in the αCD62L/αMAdCAM-1 group, whereas PP and LN regions were positive in the splenectomy plus isotype antibody group. Less intense signals projected to the BM compartment in the αCD62L/αMAdCAM-1$_{SplEx}$ group. (D) Blocking the access to SLO by αCD62L/αMAdCAM-1$_{SplEx}$ was effective as measured by ex vivo imaging (top left) and immune fluorescence microscopy (Thy1.1$^+$ donor T cells in blue, MHC II$^+$ host APCs in red, isotype control right panels). Histopathologic evaluation supported these findings, by showing a grade 2 intestinal aGVHD in isotype controls (bottom right) in comparison to unaffected GIT from the αCD62L/αMAdCAM-1$_{SplEx}$ group (bottom left). (E) All animals from the αCD62L/αMAdCAM-1$_{SplEx}$ group survived the aHCT without any signs of acute or chronic GVHD (pooled data from 3 independent experiments, $P < .001$). In contrast, αCD62L/αMAdCAM-1 treatment, isotype treatment or isotype treatment with splenectomy all resulted in acute GVHD-related mortality ($\geq$ 90%) within 70 days after aHCT. Control groups: BM only, more than 90% survival, no aGVHD; BM and splenocytes, no antibodies: 0% survival, severe aGVHD; radiation only: 0% survival.

S1, available on the *Blood* website; see the Supplemental Materials link at the top of the online article.). Thus, we concluded that SLOs are essential for the induction of aGVHD, however, there is significant redundancy of SLOs, and the spleen can give rise to gut-tropic, but also skin and liver infiltrating alloreactive T cells.

Blocking of all secondary lymphoid organs prevents aGVHD

Mice deficient for certain SLOs may develop compensatory mechanisms to cope with their immunologic impairment, as discussed for aly/aly mice and B6-LT$\alpha^{-/-}$ mice.[30,31] Thus, confounding factors such as arising tertiary or inducible lymphoid organs[32,33] may influence experimental outcome. Furthermore, remaining SLOs, such as mLN and spleen in PP^{KO} mice or the spleen in B6-LT$\alpha^{-/-}$ mice, might possibly adopt additional functions in surveying intestinal mucosal surfaces.

To rule out such a potential experimental bias, we explored short-term homing blockage of SLOs with monoclonal antibodies (MAbs). We treated aHCT recipients intravenously with blocking MAbs to L-selectin (αCD62L) or MAdCAM-1 (αMAdCAM-1), important homing ligands that facilitate the entry of lymphocytes into pLNs and PP, respectively. We found that a single injection of 150 μg αMAdCAM-1 or αCD62L at the time of aHCT did not alter the onset of aGVHD, contrary to reports of nonmyeloablative or unconditioned aHCT recipients[19] (data not shown). In addition, continual administration of either αMAdCAM-1 or αCD62L did not prevent aGVHD (data not shown). Therefore we administered combined αMAdCAM-1/αCD62L daily until day 5. BLI revealed that combined MAb delivery efficiently blocked the access to LNs and PP, as illustrated by the lack of cervical lymph node infiltration (Figure 4A). Nevertheless, aGVHD onset and organ manifestation was not altered compared with aHCT recipients that received isotype control MAbs. Splenectomized recipients receiving isotype control antibodies developed the same aGVHD target organ manifestation as controls. These data support the findings of lymphatic redundancy during aGVHD initiation in myeloablative-conditioned recipients (Table 1). This redundancy is also reflected in comparable absolute total-body BLI signal increases (Figure 4B). BLI revealed infiltration of proliferating *luc*$^+$ donor cells over the respective compensatory sites (Figure 4C). Peripheral blood chimerism analysis on day 6 in splenectomized recipients receiving isotype MAbs versus mice receiving the combination of blocking MAbs showed no difference from control animals receiving isotype MAbs only ($P > .05$; $> 90\%$ donor $CD4^+$, $CD8^+$, $> 80\%$ Mac-1/$CD11b^+$, Gr-1^+, $> 60\%$ $CD19^+$ cells; data not shown).

To prevent aGVHD, we splenectomized aHCT recipients and administered αMAdCAM-1/αCD62LMAbs (αMAdCAM-1/$\alpha CD62L_{SplEx}$). BLI signals in αMAdCAM-1/$\alpha CD62L_{SplEx}$ recipients differed markedly from all other groups and projected on BM compartments, while LN regions and the spleen area remained negative (Figure 4A,C). Ex vivo imaging and histology of the intestinal tract, LN, and spleen confirmed these results (Figure 4D). Overall BLI signal increase caused by proliferation of *luc*$^+$ donor cells (day 0 to day 6) was less in the αMAdCAM-1/$\alpha CD62L_{SplEx}$ group compared with other aHCT groups (Figure 4B). Nevertheless, conversion to full donor chimerism in these animals was similar to other groups receiving allogeneic T cells ($P > .05$, data not shown). Our data suggest that allogeneic donor T cells can find niches of proliferation other than SLOs, particularly the BM compartment. However, access to SLOs is required for aGVHD initiation.

Survival and clinical performance of allogeneic recipients receiving either single (not shown) or the combination of blocking MAbs, or splenectomy plus isotype MAbs demonstrate that all groups have a potentially better outcome compared with allogeneic recipients receiving no antibodies (Figure 4E). However, beneficial effects cannot be ascribed to the blocking of entry to a single priming site itself, because survival does not differ from aHCT recipients receiving isotype control antibodies only ($P > .05$). Remarkably, all splenectomized αMAdCAM-1/αCD62L–treated aHCT recipients survived without any signs of aGVHD (Figure 4E, $P < .001$).

Alloreactive T cells migrate to aGVHD target tissues irrespective of the initial priming site

To explore the observed redundancy of SLOs, we chose a complementary strategy to the previously described experiments. (Figure 5A). Myeloablatively conditioned Balb/c mice received transplants of allogeneic *luc*$^+$ FVB-L2G85 T cells as primary recipients. At the same time, conditioned Balb/c mice received transplants of nonluminescent allogeneic FVB/N WT T cells as future secondary recipients to simulate conditions similar to the primary recipients. On day 3 we transferred *luc*$^+$ T cells isolated from either pLNs, mLNs, or the spleen of the primary recipients into individual conditioned secondary aHCT recipients to track the migration of alloreactive T cells by BLI (Figure 5A). Phenotypic analysis of alloreactive *luc*$^+$ donor cells before the secondary transfer confirmed up-regulation of CD44 on T cells in all SLOs. As previously described, α4β7-integrin was up-regulated only in mLNs and spleen, in contrast to pLNs (compare Figure 1A and 1B). In vivo imaging of aHCT secondary recipients within 18h of cell transfer revealed alloreactive T-cell infiltration predominantly in abdominal sites, projecting to the intestinal tract and liver (Figure 5B). Importantly, *luc*$^+$ T cells targeted the intestinal tract and liver regardless of where they had been primed (Figure 5B,C). Target organ infiltration by *luc*$^+$ T cells persisted in secondary aHCT recipients and further extended to skin infiltration at later time points (Figure S2). These findings were consistent with our previous experiments in which access to SLO was essential while the localization of the priming site was not decisive in the aGVHD target organ manifestation.

Discussion

Several reports have provided evidence in favor of an instructive model of effector T-cell trafficking.[7-12,14,16,17] Such a model was particularly appealing as an explanation for the organ specific aGVHD manifestation mediated by donor T cells. Host antigen-presenting cells[15] initiate the alloreactive T-cell response in SLOs[2,6]; however, once activated, effector $CD4^+$ and $CD8^+$ T cells can target aGVHD organs independent of antigen recognition.[34]

Here we demonstrate that the lack of certain priming sites resulted neither in reduced nor delayed aGVHD in target tissues and that single remaining priming sites were sufficient for aGVHD induction. These observations were made in 4 independent experimental models: recipients without PP, recipients lacking PP and LN, splenectomized recipients, and recipients receiving MAbs blocking PP and LN entry or a combination of PP blocking MAbs and splenectomy. Only the prevention of access to all SLOs inhibited aGVHD target infiltration and pathology. Such abrogation was observed in splenectomized B6-LT$\alpha^{-/-}{}_{SplEx}$ recipients lacking all SLOs, or by using αMAdCAM-1 and αCD62L blocking MAbs in splenectomized Balb/c recipients. Alloreactive T cells that had

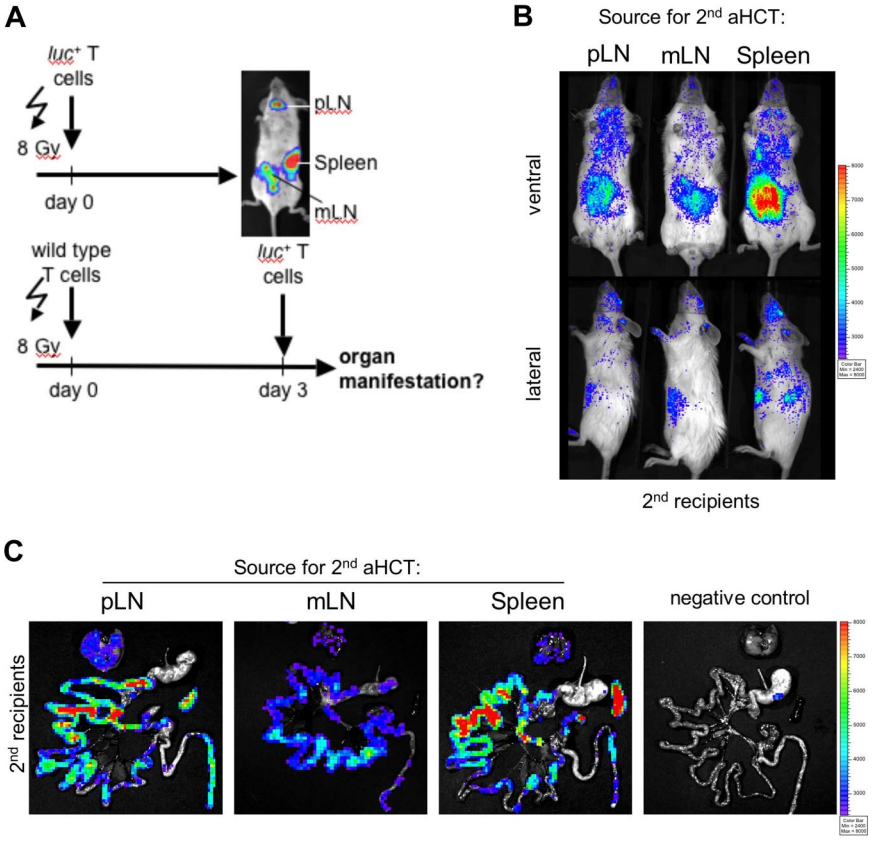

Figure 5. Intestinal and hepatic recruitment of alloreactive effector cells after transfer of in vivo primed alloreactive T cells into conditioned secondary allogeneic recipients irrespective of the original priming site. (A) Primary and secondary Balb/c (H-2^d) recipients were conditioned (2 × 4 gy) and received transplants of either *luc*$^+$ or wild-type allogeneic FVB/N (H-2^b) T cells, respectively, to simulate comparable conditions in both groups. On day 3, *luc*$^+$ T cells were isolated from either pLN (cLN and iLN combined) or mLN, or spleen. Subsequently, these in vivo primed alloreactive donor T cells were injected separately into secondary recipients to track their in vivo short-term homing. (B) Within 18 hours after secondary transfer, *luc*$^+$ T cells predominantly homed to abdominal sites in all of the analyzed groups (1 of 5 representative experiments is shown). (C) Ex vivo imaging confirmed that alloreactive *luc*$^+$ donor cells homed to the gastrointestinal tract (GIT), the liver (above GIT), and the spleen (right from GIT) in conditioned secondary recipients irrespective whether in vivo priming occurred in pLN, mLN, or spleen.

been isolated from different priming sites, namely mLN, pLN, or spleen, and transferred into secondary conditioned recipients rapidly infiltrated the intestinal tract and liver irrespective of their original priming sites. Although alloreactive CD4$^+$ and CD8$^+$ T cells in pLN expressed low levels of α4β7 integrin, αEβ7 integrin or CCR9, these cells homed to the intestinal tract and liver as effectively as cells from mLN. Lastly, transferred alloreactive effector cells primed in the spleen also homed efficiently to intestines and liver.

In accordance with prior studies, we found that homing receptor acquisition in SLO is nonstochastic. Yet other receptors such as CD44, and to a lesser extent P-selectin ligand, were up-regulated on donor T cells infiltrating all SLOs. CD44 and P-selectin ligands are functionally implicated in effector lymphocyte trafficking to inflamed tissues.[35,36] Clinical aHCT involves conditioning regimens of the recipient to eradicate residual disease in cancer patients and to provide immunologic acceptance of the graft. To model the clinical situation, our aHCT experiments also involved host conditioning before transplantation. Inflammatory cytokine release, including tumor necosis factor (TNF) α and IL-1, following the conditioning regimen and the GVH reaction, can accelerate aGVHD onset.[1,34,37,38] Conversely, neutralizing TNFα and IL-1 prevented aGVHD in CD4$^+$- and CD8$^+$-dependent models.[34] Importantly, blocking these cytokines did not affect aGVHD initiation, but the aGVHD effector-phase, resulting in reduced intestinal and hepatic alloreactive T-cell infiltration. Moreover, precise timing and dosing of this treatment strategy seemed essential, because other investigators could not observe the same beneficial effects using a similar approach.[39,40] These data strongly suggest that TNFα and IL-1, together with effects further downstream, are pivotal in rendering aGVHD target organs permissible for alloreactive T-cell infiltration as opposed to non-GVHD targets. In fact, intercellular adhesion molecule (ICAM)-1 and vascular cell adhesion molecule (VCAM)-1, facilitating T-cell entry into aGVHD targets, are up-regulated upon host conditioning.[41] Our strategy of MAdCAM-1 blocking could not reproduce the same beneficial effects as transfer of allogeneic α4β7$^-$ T cells to reduce intestinal aGVHD.[42] It remains possible that in our study, VCAM-1 or other α4β7-ligands induced upon host conditioning on intestinal vascular endothelial cells compensated for MAdCAM-1 blocking. Induced adhesion molecules can also enhance retention of alloreactive effector T cells, as it has been shown for TGF-β and αEβ7 integrin (CD103) expression on alloreactive T cells in the intestinal tract.[26]

Murai et al described aGVHD protection in PP^{KO} recipients within the first 30 days after aHCT using a non- or reduced-conditioning haploidentical transplant model.[19] In contrast, we could not observe the same beneficial effects in our aHCT model preventing access to PP or other selected lymphoid organs. Similarly, Clouthier et al observed aGVHD organ manifestation in splenectomized recipients[43] and Welniak et al in PP^{KO} mice.[29] Using our BLI model we could visualize that accessible SLOs can compensate for nonaccessible SLOs. This redundancy of SLOs in aGVHD initiation is further supported by our observations from secondary transfer experiments, in which alloreactive T cells infiltrate aGVHD target tissues irrespective of the initial priming site. Therefore, the type and the intensity of conditioning regimens used in aHCT studies must be taken into consideration. Highlighting such differences in an inflammatory versus noninflammatory environment, a study by Wysocki et al uncovered different roles for CCR5 by comparing unconditioned (reduced GVHD[19,44]) with conditioned aHCT recipients (exacerbated aGVHD by CCR5$^{-/-}$ donor T cells).[45]

An intriguing result from our study is that the combined αMAdCAM-1/αCD62L treatment plus splenectomy entirely prevented aGVHD. This is surprising, because we expected a delayed aGVHD onset when we stopped administration of αMAdCAM-1 and αCD62L on day 5 after aHCT. As reported in models of delayed donor lymphocyte infusion (DLI),[46] inflammatory responses due to host conditioning decline in the absence of alloreactive T cells, which could not access SLOs during the first week after aHCT. As interactions between activated host-APCs with donor T cells are essential for aGVHD initiation,[15] donor chimerism conversion could have reduced efficient host-APC-alloreactive T-cell interactions by the time of SLO entry. Supporting this concept was a high $CD11b^+$ donor cell chimerism by day 6. In addition, by the time alloreactive T-cell clones could finally access SLOs, regulatory immune mechanisms could have regained control while simultaneously inflammatory responses due the host conditioning have declined. In line with this, reducing the toxicity of conditioning regimens for aHCT holds great promise as reported for the combination therapy of total lymphoid irradiation and antithymocyte serum that reduced aGVHD incidence in humans.[47]

In conclusion, our study demonstrates that access to SLOs is essential in aGVHD initiation. Importantly, we have shown that multiple redundant priming sites exist throughout the body. Blocking access to all SLOs is required to prevent the onset of aGVHD.

Acknowledgments

We thank Dr Jeff Browning from Biogen for the generous gift of LTβR-IgG fusion protein, Carolin Kiesel for expert assistance, Dr Tim Doyle and Dick Stovel for technical expertise, and Dr Pia Bjorck and the members of the Negrin, Contag, and Butcher laboratories for constructive discussions.

This work was supported by a Supergen Postdoctoral Fellowship of the Amy Strelzer-Manasevit Research Program of the National Marrow Donor Program (NMDP) (A.B.), by a grant from the Interdisciplinary Center for Clinical Research (IZKF) Würzburg, Germany (A.B.), by a fellowship of the Akademie der Naturforscher Leopoldina (S.S.), and grants from the National Institutes of Health (R24CA92862, RO1CA80006, PO1CA49605, and R33CA88303).

Authorship

Contribution: A.B. and S.S. designed and performed research, contributed new reagents, analyzed data, and wrote the paper. J.B. and G.F.B. designed and performed research and helped write the paper. R.N., G.L., E.M.B. and E.I.H. performed research, analyzed data, and helped write the paper. E.C.B. contributed vital reagents. C.H.C. contributed vital reagents and analytical tools. R.S.N. designed research and helped write the paper.

Conflict-of-interest disclosure: The authors declare no competing financial interests

Correspondence: Robert S. Negrin, MD, Center for Clinical Sciences Research Building, Room 2205, 269 W Campus Drive, Stanford, CA 94305; e-mail: Negrs@stanford.edu.

References

1. Ferrara JL, Deeg HJ. Graft-versus-host disease. N Engl J Med. 1991;324:667-674.
2. Beilhack A, Schulz S, Baker J, et al. In vivo analyses of early events in acute graft-versus-host disease reveal sequential infiltration of T-cell subsets. Blood. 2005;106:1113-1122.
3. Miller MJ, Wei SH, Parker I, Cahalan MD. Two-photon imaging of lymphocyte motility and antigen response in intact lymph node. Science. 2002;296:1869-1873.
4. Stoll S, Delon J, Brotz TM, Germain RN. Dynamic imaging of T cell-dendritic cell interactions in lymph nodes. Science. 2002;296:1873-1876.
5. Mempel TR, Henrickson SE, Von Andrian UH. T-cell priming by dendritic cells in lymph nodes occurs in three distinct phases. Nature. 2004;427:154-159.
6. Panoskaltsis-Mortari A, Price A, Hermanson JR, et al. In vivo imaging of graft-versus-host-disease in mice. Blood. 2004;103:3590-3598.
7. Guy-Grand D, Griscelli C, Vassalli P. The mouse gut T lymphocyte, a novel type of T cell. Nature, origin, and traffic in mice in normal and graft-versus-host conditions. J Exp Med. 1978;148:1661-1677.
8. Campbell DJ, Butcher EC. Rapid acquisition of tissue-specific homing phenotypes by CD4(+) T cells activated in cutaneous or mucosal lymphoid tissues. J Exp Med. 2002;195:135-141.
9. Stagg AJ, Kamm MA, Knight SC. Intestinal dendritic cells increase T cell expression of alpha4beta7 integrin. Eur J Immunol. 2002;32:1445-1454.
10. Mora JR, Bono MR, Manjunath N, et al. Selective imprinting of gut-homing T cells by Peyer's's patch dendritic cells. Nature. 2003;424:88-93.
11. Johansson-Lindbom B, Svensson M, Wurbel MA, Malissen B, Marquez G, Agace W. Selective generation of gut tropic T cells in gut-associated lymphoid tissue (GALT): requirement for GALT dendritic cells and adjuvant. J Exp Med. 2003;198:963-969.
12. Stenstad H, Ericsson A, Johansson-Lindbom B, et al. Gut-associated lymphoid tissue-primed CD4+ T cells display CCR9-dependent and -independent homing to the small intestine. Blood. 2006;107:3447-3454.
13. Agace WW. Tissue-tropic effector T cells: generation and targeting opportunities. Nat Rev Immunol. 2006;6:682-692.
14. Picker LJ, Treer JR, Ferguson-Darnell B, Collins PA, Bergstresser PR, Terstappen LW. Control of lymphocyte recirculation in man. II. Differential regulation of the cutaneous lymphocyte-associated antigen, a tissue-selective homing receptor for skin-homing T cells. J Immunol. 1993;150:1122-1136.
15. Shlomchik WD, Couzens MS, Tang CB, et al. Prevention of graft versus host disease by inactivation of host antigen-presenting cells. Science. 1999;285:412-415.
16. Johansson-Lindbom B, Svensson M, Pabst O, et al. Functional specialization of gut CD103+ dendritic cells in the regulation of tissue-selective T cell homing. J Exp Med. 2005;202:1063-1073.
17. Mora JR, Cheng G, Picarella D, Briskin M, Buchanan N, von Andrian UH. Reciprocal and dynamic control of CD8 T cell homing by dendritic cells from skin- and gut-associated lymphoid tissues. J Exp Med. 2005;201:303-316.
18. Iwata M, Hirakiyama A, Eshima Y, Kagechika H, Kato C, Song SY. Retinoic acid imprints gut-homing specificity on T cells. Immunity. 2004;21:527-538.
19. Murai M, Yoneyama H, Ezaki T, et al. Peyer's's patch is the essential site in initiating murine acute and lethal graft-versus-host reaction. Nat Immunol. 2003;4:154-160.
20. Davenport MP, Grimm MC, Lloyd AR. A homing selection hypothesis for T-cell trafficking. Immunol Today. 2000;21:315-317.
21. De Togni P, Goellner J, Ruddle NH, et al. Abnormal development of peripheral lymphoid organs in mice deficient in lymphotoxin. Science. 1994;264:703-707.
22. Rennert PD, James D, Mackay F, Browning JL, Hochman PS. Lymph node genesis is induced by signaling through the lymphotoxin beta receptor. Immunity. 1998;9:71-79.
23. Rennert PD, Browning JL, Hochman PS. Selective disruption of lymphotoxin ligands reveals a novel set of mucosal lymph nodes and unique effects on lymph node cellular organization. Int Immunol. 1997;9:1627-1639.
24. Cao YA, Wagers AJ, Beilhack A, et al. Shifting foci of hematopoiesis during reconstitution from single stem cells. Proc Natl Acad Sci U S A. 2004;101:221-226.
25. Cao YA, Bachmann MH, Beilhack A, et al. Molecular imaging using labeled donor tissues reveals patterns of engraftment, rejection, and survival in transplantation. Transplantation. 2005;80:134-139.
26. El-Asady R, Yuan R, Liu K, et al. TGF-{beta}-dependent CD103 expression by CD8(+) T cells promotes selective destruction of the host intestinal epithelium during graft-versus-host disease. J Exp Med. 2005;201:1647-1657.
27. Kunkel EJ, Campbell JJ, Haraldsen G, et al. Lymphocyte CC chemokine receptor 9 and epithelial thymus-expressed chemokine (TECK) expression distinguish the small intestinal immune compartment: Epithelial expression of tissue-specific chemokines as an organizing principle in regional immunity. J Exp Med. 2000;192:761-768.
28. Svensson M, Marsal J, Ericsson A, et al. CCL25 mediates the localization of recently activated CD8alphabeta(+) lymphocytes to the small-intestinal mucosa. J Clin Invest. 2002;110:1113-1121.
29. Welniak LA, Kuprash DV, Tumanov AV, et al. Peyer's patches are not required for acute graft-versus-host disease after myeloablative conditioning and murine allogeneic bone marrow transplantation. Blood. 2006;107:410-412.
30. Lakkis FG, Arakelov A, Konieczny BT, Inoue Y. Immunologic 'ignorance' of vascularized organ

transplants in the absence of secondary lymphoid tissue. Nat Med. 2000;6:686-688.

31. Chin R, Zhou P, Alegre ML, Fu YX. Confounding factors complicate conclusions in aly model. Nat Med. 2001;7:1165-1166.
32. Fütterer A, Mink K, Luz A, Kosco-Vilbois MH, Pfeffer K. The lymphotoxin beta receptor controls organogenesis and affinity maturation in peripheral lymphoid tissues. Immunity. 1998;9:59-70.
33. Moyron-Quiroz JE, Rangel-Moreno J, Kusser K, et al. Role of inducible bronchus associated lymphoid tissue (iBALT) in respiratory immunity. Nat Med. 2004;10:927-934.
34. Teshima T, Ordemann R, Reddy P, et al. Acute graft-versus-host disease does not require alloantigen expression on host epithelium. Nat Med. 2002;8:575-581.
35. DeGrendele HC, Estess P, Siegelman MH. Requirement for CD44 in activated T cell extravasation into an inflammatory site. Science. 1997;278:672-675.
36. Haddad W, Cooper CJ, Zhang Z, et al. P-selectin and P-selectin glycoprotein ligand 1 are major determinants for Th1 cell recruitment to nonlymphoid effector sites in the intestinal lamina propria. J Exp Med. 2003;198:369-377.
37. Holler E, Kolb HJ, Moller A, et al. Increased serum levels of tumor necrosis factor alpha precede major complications of bone marrow transplantation. Blood. 1990;75:1011-1016.
38. Hill GR, Teshima T, Gerbitz A, et al. Differential roles of IL-1 and TNF-alpha on graft-versus-host disease and graft versus leukemia. J Clin Invest. 1999;104:459-467.
39. Hattori K, Hirano T, Miyajima H, et al. Differential effects of anti-Fas ligand and anti-tumor necrosis factor alpha antibodies on acute graft-versus-host disease pathologies. Blood. 1998;91:4051-4055.
40. Piguet PF, Grau GE, Allet B, Vassalli P. Tumor necrosis factor/cachectin is an effector of skin and gut lesions of the acute phase of graft-vs.-host disease. J Exp Med. 1987;166:1280-1289.
41. Eyrich M, Burger G, Marquardt K, et al. Sequential expression of adhesion and costimulatory molecules in graft-versus-host disease target organs after murine bone marrow transplantation across minor histocompatibility antigen barriers. Biol Blood Marrow Transplant. 2005;11:371-382.
42. Petrovic A, Alpdogan O, Willis LM, et al. LPAM (alpha 4 beta 7 integrin) is an important homing integrin on alloreactive T cells in the development of intestinal graft-versus-host disease. Blood. 2004;103:1542-1547.
43. Clouthier SG, Ferrara JL, Teshima T. Graft-versus-host disease in the absence of the spleen after allogeneic bone marrow transplantation. Transplantation. 2002;73:1679-1681.
44. Murai M, Yoneyama H, Harada A, et al. Active participation of CCR5(+)CD8(+) T lymphocytes in the pathogenesis of liver injury in graft-versus-host disease. J Clin Invest. 1999;104:49-57.
45. Wysocki CA, Jiang Q, Panoskaltsis-Mortari A, et al. Critical role for CCR5 in the function of donor CD4+CD25+ regulatory T cells during acute graft-versus-host disease. Blood. 2005;106:3300-3307.
46. Chakraverty R, Cote D, Buchli J, et al. An inflammatory checkpoint regulates recruitment of graft-versus-host reactive T cells to peripheral tissues. J Exp Med. 2006;203:2021-2031.
47. Lowsky R, Takahashi T, Liu YP, et al. Protective conditioning for acute graft-versus-host disease. N Engl J Med. 2005;353:1321-1331.